

Carbonate redistribution and hydrogeochemical processes in two calcareous soils with groundwater in a Mediterranean environment

R. BOUZIGUES^a, O. RIBOLZI^b, J.C. FAVROT^a & V. VALLES^b

^aLaboratoire de Science du Sol, INRA, 2 place Viala, 34060 Montpellier Cedex 1; and ^bLaboratoire de Science du Sol, INRA, Domaine Saint-Paul, Site Agroparc 84914 Avignon Cedex 9, France

Summary

The morphology of the soil is closely associated with water regime and redistribution of solutes. We studied in detail two calcareous soils with groundwater representative of the two main hydrogeological regimes, one on the plateau and the other in the central depression, of an experimental catchment near Roujan in the South of France. We recorded macro- and micromorphological features, and measured the level of the water table and the saturating solution. The morphological features were primarily those associated with carbonate redistribution. The forms associated with iron and manganese added information. The two groundwater systems behaved differently over 3 years. The temporary perched groundwater of the plateau was characterized by a small partial pressure of CO₂ ($p\text{CO}_2$) and a large $p\text{O}_2$, with rapid lowering of the water table (4–6 cm d⁻¹). The permanent groundwater of the depression, in contrast, had a larger $p\text{CO}_2$ and a small $p\text{O}_2$. The water table fell more slowly (1–2 cm d⁻¹). Higher up, rapid drying of the profile and release of CO₂ leads to over-saturation of the soil solution with respect to calcite, favouring the formation of poorly crystallized micrites, which are characteristic of the plateau system. In the lower part of the catchment, persistent waterlogging leads to more marked anaerobiosis (large estimated $p\text{CO}_2$) favouring the development of large stable rhombohedral crystals characteristic of more stable hydrodynamic conditions. In both situations, iron and more particularly manganese redistribution agrees with the waterlogged state of these soils.

Redistribution des carbonates et fonctionnement hydrogéochimique de deux sols calcaires à nappe en milieu méditerranéen

Résumé

Il existe des liens étroits entre les traits morphologiques liés à la redistribution des éléments chimiques dans les sols et la cinétique des nappes. Cette étude porte sur l'analyse détaillée de deux profils de sols calcaires à nappe représentatifs des deux principaux ensembles hydrogéologiques—plateau et dépression—d'un bassin versant expérimental près de Roujan au sud de la France. Ces profils ont fait l'objet d'observations macro et micromorphologiques, de suivis piézométriques et d'une caractérisation physico-chimique de la solution saturante. Les analyses morphologiques concernent surtout les traits liés à la redistribution des carbonates, les formes associées au fer et au manganèse étant analysées à titre complémentaire. Trois années de suivi piézométrique montrent que les deux systèmes de nappe présents ont des comportements très contrastés. La nappe perchée temporaire du plateau caractérisée par une pression de CO₂ ($p\text{CO}_2$) estimée faible et une $p\text{O}_2$ forte, présente des vitesses de rabattement rapide (4 à 6 cm j⁻¹). La nappe permanente de la dépression en aval présente au contraire une $p\text{CO}_2$ plus importante et une $p\text{O}_2$ faible. Les vitesses de rabattement y sont plus faibles que précédemment (1 à 2 cm j⁻¹). En amont, le dessèchement

rapide du profil et le dégazage du CO₂ conduit à une sursaturation de la solution du sol par rapport à la calcite, ce qui favorise la formation de micrites mal cristallisés, caractéristiques de ce premier système. Dans le bas fond, la persistance de l'engorgement entraîne une anaérobiose plus marquée ($p\text{CO}_2$ forte) et favorise le mûrissement de gros cristaux rhomboédriques caractéristiques de conditions hydrodynamiques plus stables. Enfin, dans les deux situations, les redistributions du fer et surtout du manganèse confirment l'engorgement de ces sols.

Introduction

Redistribution of the chemical elements in soils with excess water is associated both with weathering and neoformation and with flowing water, which may displace the products formed. These mechanisms can be regarded in two ways. There is a naturalistic approach which deduces the processes responsible for redistribution of the elements from their macro- and micromorphological characteristics (e.g. Crown & Hoffman, 1970; Fanning *et al.*, 1973; Van Vallemburg, 1973; Vizier, 1974). The second, deterministic approach involves modelling and simulation of processes to predict the factors likely to affect redistribution, for instance by combining the transfer of water and solutes in the same model (e.g. Rieux, 1978; Valles, 1987; Marlet, 1996).

The first approach indicates overall soil water regime. Conversely, knowledge of water flow kinetics and the paths the water takes give a better understanding of the origin of certain morphological features. Most research in this field focuses on modes of iron redistribution in acid hydromorphic soils in temperate climates (Evans & Franzmeier, 1988; Faulkner & Patrick, 1992; Patrick & Jugsujinda, 1992; Mokma & Sprecher, 1994a,b; Soulier, 1995) or tropical ones (Vizier, 1989). In contrast, there have been few studies on forms associated with carbonate redistribution (Hardan & Abbas, 1973; Bouzigues *et al.*, 1992), particularly in Mediterranean conditions. There are several modes of carbonate redistribution, because of the variety of processes that can be involved. The latter may be biological, the formation of calcitized cells, for instance (e.g. Jaillard *et al.*, 1991), chemical (e.g. Delmas *et al.*, 1987), with surface dissolution of carbonate minerals, or purely physical, as a result of drying in arid or Mediterranean environments (e.g. Kaemmerer *et al.*, 1991; Kaemmerer & Revel, 1996). In the latter case, drying can lead to more or less rapid over-saturation, which may affect the size and degree of crystallinity of the crystals (e.g. Al-Droubi, 1976).

We have examined the relations between the forms of carbonate redistribution and the water regime of calcareous hydromorphic soils in a Mediterranean environment. We have characterized the morphology of the soils and examined the crystalline structure of the redistributed carbonate and compared them with piezometric measurements and the physico-chemical characteristics of the saturating water. The modes of iron and manganese redistribution are briefly examined to complement information derived from the carbonate-related features. Observations and measurements were made at many

sites in the experimental catchment of the ALLEGRO-Roujan multidisciplinary research programme. The results presented here are based on two representative profiles of calcareous soils with contrasting hydrological behaviour.

Environment, materials and methods

The Roujan experimental catchment

The 90-ha Roujan catchment (Andrieux *et al.*, 1993) is on the Languedoc plain 60 km north-west of Montpellier. For many decades it has been almost entirely under vines. It has a subhumid Mediterranean climate with a long dry season. The mean annual rainfall (650 mm) masks great differences both within years and from year to year. Rain is generally heaviest in October and February. The mean annual temperature is 14°C, and the mean temperature of the hottest month, July, is 23°C. Potential evapotranspiration, intensified by frequent winds, exceeds 1000 mm with daily peaks of up to 5 mm (Trambouze, 1996).

The catchment can be divided into four sectors (Fig. 1): the plateau rising to 120 m, the terraced slopes, the gentle colluvial footslope, and the central depression 80 m above sea level. The plateau bears mainly stony red soil with secondary carbonates (Chromic Luvisol with secondary carbonates, FAO, 1988). The clay soil of the slopes is calcareous and is locally affected by seasonal springs, giving rise to Calcic Gleysols. The footslope is mantled by calcareous soil with a weakly differentiated profile (Calcisols). The soil of the central depression is of medium to fine texture and characterized by redox mottles (Calcic Gleysol).

Two spatially differentiated systems of unconfined water were identified: the temporary groundwater of the plateau, which feeds the springs at the top of the slopes, and the permanent groundwater system of the footslope-depression sector.

Observations and pedological analysis

The results presented here are from two sites. We selected them after examining the records of the 500 auger boreholes and 60 profile pits used for the survey of the Roujan catchment (Andrieux *et al.*, 1993). The two represent contrasting hydrological conditions. One is on the plateau (P1), the other in the central depression near the catchment's outlet (P2). Observations made on the nonhydromorphic soil of the footslope are also presented for comparison.

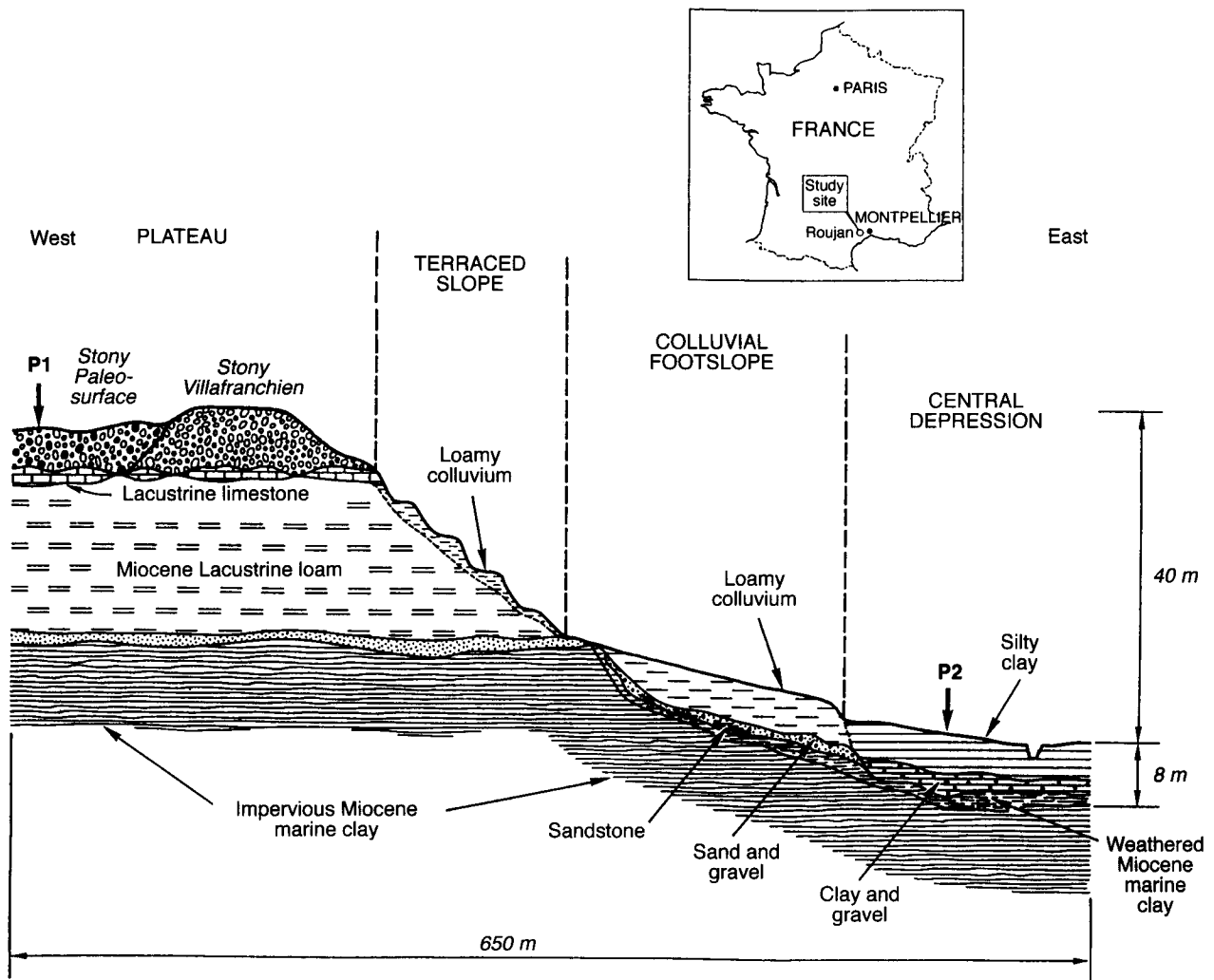


Fig. 1 Site location and cross-section of the experimental catchment (Andrieux *et al.*, 1993).

To characterize the morphological features associated with the hydromorphy we took cubic blocks of undisturbed soil with 10- to 12-cm sides from the various horizons at depths down to about 2 m. The features indicating water excess were described using a binocular microscope ($\times 8$ to $\times 30$ magnification), then a scanning electron microscope (SEM, $\times 500$ to $\times 10\,000$ magnification). The elements Fe, Ti, Mn, K, Ca, Mg, Si, Al in the morphological features were measured using an electron microprobe linked to the SEM. Finally, the crystalline nature of the features was examined by ray diffractometry.

Hydrological monitoring

Piezometric measurements were made on 15 sites (more than 40 piezometers). Only readings taken close to the two profiles P1 and P2 and on the footslope are reported here. Measurements were made over 610 days (October 1992 to April 1995), during which the rainfall was normal for the time of year. Each site is equipped with four PVC tubes, 5 cm in diameter,

positioned at depths of between 1 and 5 m. The part of each tube above the screen is encased in bentonite to prevent water infiltrating down the side of the piezometer. Automatic readings are taken at hourly intervals using ultrasonic sensors accurate to between 0.5 and 1 cm. Four rain recorders and nine rain gauges are distributed over the whole of the catchment.

Groundwater samples and analysis

Groundwater samples were collected during 1992 and 1993 to establish the physicochemical characteristics of the groundwater and to examine their state of saturation with respect to the minerals present in the soil. Samples were taken from piezometers and wells over the whole of the catchment (Ribolzi *et al.*, 1993) and close to profiles P1 and P2.

The pH, Eh (redox potential) and temperature were measured *in situ*. Samples were stored in the dark at 4°C in polyethylene flasks after microfiltration at 0.45 µm. The Cl^- , Na^+ and NO_3^- ions were measured by selective electrode

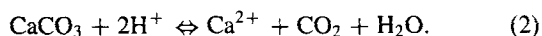
(ORION 84-11, 94-17B and 93-07) in conjunction with an ionic strength adjuster and interference suppressor. The NO_3^- ions were determined within 24 h. Total concentrations of K^+ , Ca^{2+} and Mg^{2+} were determined by atomic absorption spectrometry (PERKIN-ELMER, 2100), whilst sulphur was analysed by plasma emission (JOBIN-YVON, JY24). Finally, carbonate alkalinity (i.e. carbonate Acid-Neutralizing-Capacity) was measured by acid titration using the Gran method (Gran, 1952) with return titration by NaOH (Vorob'yeva & Zamana, 1984; Keller *et al.*, 1987).

Theoretical tools and thermodynamic model

When a soil is saturated with water gaseous exchange with the atmosphere is reduced (e.g. Sierra *et al.*, 1995). This affects the pressure of the carbon dioxide in the soil and increases the solubility of the carbonate minerals. In the case of interactions between calcite and the soil solution the saturation state of the solution can be determined using the following formula for calculating the degree of saturation (S_{calcite}):

$$S_{\text{calcite}} = \log \frac{Q}{K_{\text{calcite}}^{285 \text{ K}}}, \quad (1)$$

where Q is the product of ionic activity of the solution, and $K_{\text{calcite}}^{285 \text{ K}}$ is the solubility product of calcite (CaCO_3) at 285 K (the average temperature of the groundwater). If $S_{\text{calcite}} > 0$ the solution is over-saturated in relation to the mineral; and if $S_{\text{calcite}} < 0$ it is under-saturated. In other words, $\log K_{\text{calcite}}^{285 \text{ K}} = 9.59$ (Helgeson, 1969; Helgeson *et al.*, 1971) if we consider the equilibrium:



The theoretical solubility product, $\log K_{\text{calcite}}^{285 \text{ K}} = 9.59$, corresponds to a mineral that is completely pure, ideally crystallized and of infinite size. With small grains, the interfacial energy of the solid-liquid interface becomes significant (Defay & Prigogine, 1951) and solubility increases in accordance with Ostwald-Freundlich's law:

$$\ln \left(\frac{[K_{\text{M}}^T]_r}{[K_{\text{M}}^T]_\infty} \right) = - \frac{kv\sigma}{RT}, \quad (3)$$

in which $[K_{\text{M}}^T]_\infty$ is the solubility of a mineral M of infinite size at absolute temperature T , $[K_{\text{M}}^T]_r$ is the solubility of a mineral M of radius r , k is the form factor of the solid, v is the molar volume of the solid, σ is the surface energy of the solid, T is the absolute temperature, and R is the perfect gas constant.

The solubility of the mineral thus approaches infinity as the theoretical radius approaches zero. Research into the growth of crystals and nucleation shows that the latter is triggered at a high solubility $[K_{\text{M}}^T]_{r_c}$ corresponding to a critical radius (r_c) in accordance with the following equation:

$$\ln \left(\frac{[K_{\text{M}}^T]_{r_c}}{[K_{\text{M}}^T]_\infty} \right) = - \frac{kv\sigma}{RT r_c}. \quad (4)$$

Nucleation is thus possible only with large S_{calcite} values and leads to the formation of small crystals.

We calculated the saturation states of the solutions with respect to calcite using the AQUA software ion-pair model of Valles & De Cockborne (1992). This model is derived from the GYPSOL program of Valles (1987) and Valles & Bourgeat (1988), based on the Debye-Hückel law including the deviation function of Scatchard. Equilibrium (2) indicates that the solubility of calcite is associated with the partial pressure of carbon dioxide ($p\text{CO}_2$). The redox processes are likewise linked to oxidation in the soil. The equilibrating pressures of the CO_2 and O_2 ($p\text{O}_2$) were evaluated with the AQUA software. The pressure $p\text{CO}_2$ was calculated using the pH measurement in the field and the carbonate alkalinity of each solution (Bourri , 1976; Keller *et al.*, 1987), and $p\text{O}_2$ was evaluated using the Eh and pH measurements (e.g. Fritz, 1981; Garcia, 1996).

Results

Forms of carbonate mineral redistribution

Secondary precipitation of carbonates is abundant in the plateau soil from 50 cm downwards (Fig. 2). It takes the form of thin white coatings around numerous aggregates and small weathered crystals of calcite less than 5 μm across (Fig. 3). Rhizomorphic structures in the form of calcified cells about 50 μm across occupy numerous root pores (Fig. 3). On the plateau the inherited carbonates (Fig. 2) consist of pebbles and stones, some of which weather into a fine white powder. They differ from the secondary carbonates in that they are fairly evenly distributed in the various horizons and that there are well crystallized crystals of average size (20–50 μm) present.

Calcite appears in two main forms in the soil of the depression. Whitish pseudomycelia consisting of calcitized cells 50–100 μm in size (Fig. 3) are present from 50 cm downwards (Fig. 2) and abound in the grey horizon between 100 and 160–180 cm. Below 160–180 cm yellowish-white nodules appear, several centimetres in diameter, some of which are composed of rhombohedrons of well crystallized calcite which may exceed 200 μm (Fig. 3). A few small crystals, several micrometres in size and of very variable shape, are associated with them.

The nonwaterlogged footslope soil contains only a few whitish threads formed from calcified root cells, 50–100 μm in size. They develop occasionally within compacted prisms of the cambic horizon structure.

Manganese- and iron-related morphology

The morphological features associated with manganese redistribution are common in both sectors. On the plateau these essentially consist of blackish pellicular coatings several

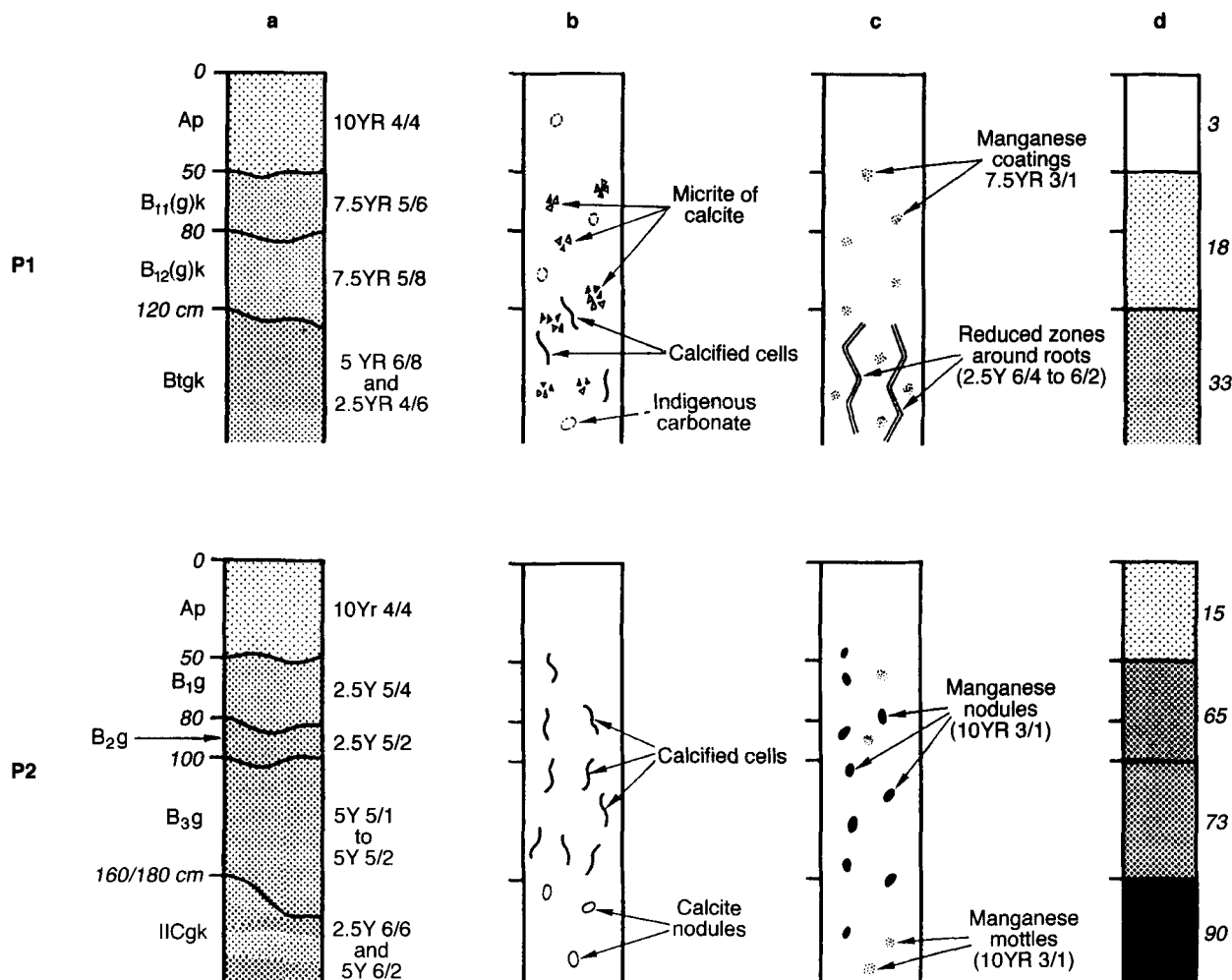


Fig. 2 Schematic profiles on the plateau (P1) and depression (P2): (a) morphology, (b) carbonates, (c) iron and manganese, and (d) duration of saturation (time of presence of groundwater in percentage of total time—610 days—of piezometric measurements).

millimetres in size on the reddish faces of some aggregates. These deposits were observed from 50 cm downwards and are slightly larger and more frequent below 120 cm. Manganese appears in the depression almost exclusively in small blackish, friable nodules (1–5 mm in diameter). Although rare at the top of the profile, these nodules are abundant in the 80–160-cm horizon. In both situations these coatings or nodules consist of 50–60% noncrystalline manganese (Fig. 4) and are arranged as flaky aggregates (Fig. 3).

Movement of iron is apparent on the plateau below 120 cm. There are zones depleted of iron around roots and around some aggregates. In the soils in the depression, the movement of iron can be identified by the presence of a few weakly contrasted rusty spots several millimetres in diameter and by the very faint colour of the matrix between 80 and 160–180 cm (chroma value; 2 or under).

The footslope soils have few iron and manganese mottles and nodules, in contrast to the two reference profiles.

Water table dynamics

The recharge of the water table beneath the plateau is similar to that in the depression (Fig. 5). It rises rapidly after the autumn rains, by up to 2 m d^{-1} . The rate at which the water table falls, on the other hand, depends on the particular location, with considerable variation in the time during which the soil is saturated (Fig. 6).

The water table of the plateau fell rapidly and steadily (Fig. 5), at $4\text{--}6 \text{ cm d}^{-1}$, as soon as the rain stopped, remaining above 1 m depth for 18% of the total period of piezometric measurements and above 2 m for 33% of the period (Fig. 2). The water table in the depression initially dropped rapidly to 0.5 m depth, then remained at between 0.5 and 1 m until mid-June. The rate of lowering varied between 1 and 2 cm d^{-1} during this period. In the summer the water table gradually fell to 3 m, and it remained between 0 and 0.5 m for 15% and between 0.5 and 1 m for 73% of the 30 months (Fig. 2). The

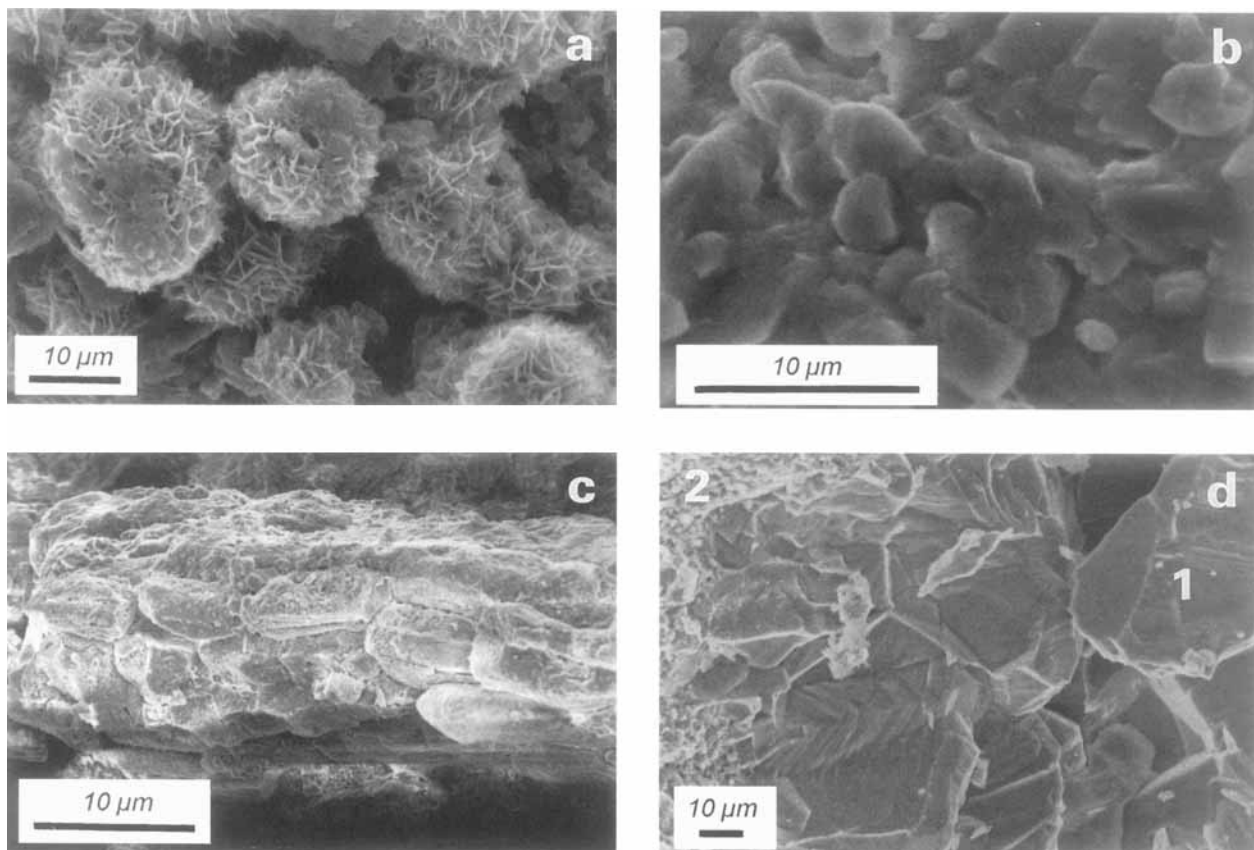


Fig. 3 View of morphological features with scanning electron microscope: (a) black nodule rich in manganese (P2, depth 110 cm), (b) whitish concentration of calcite (P1, depth 120 cm), (c) calcified roots cells (P2, depth 80 cm), (d) calcareous nodule with large (1) and small (2) crystals of calcite (P2, depth 170 cm).

water table beneath the footslope rarely rose above the 3 m level (Fig. 5).

Geochemical characteristics of the groundwaters

The estimated $p\text{CO}_2$ of the groundwater of the depression (up to 100 times atmospheric $p\text{CO}_2$) was larger than that of the plateau (Ribolzi *et al.*, 1993) (Fig. 7). This difference was also observed for the two representative sites P1 and P2 (Table 2).

The groundwater was mainly over-saturated with respect to calcite (Fig. 7) and over-saturation increased as the $p\text{CO}_2$ declined. A greater over-saturation was thus observed on the plateau, where the $p\text{CO}_2$ was smaller. In addition, in contrast to the $p\text{CO}_2$, the equilibrating $p\text{O}_2$ was less on the plateau (Table 2).

All Eh-pH pairs are within the stability range for ferric iron (Fig. 8). The groundwater in the lower part of the catchment is more reducing than that of the plateau without, however, reaching equilibrium between ferrous and ferric iron. In both cases, most measurements were in the manganese reduction range (Fig. 9), indicating that the manganese oxides are soluble.

Discussion

The soil of the plateau

The rapid lowering of the water table on the plateau explains the moderate nature of the anaerobic conditions, characterized by a small estimated $p\text{CO}_2$. The pore space thus liberated re-establishes gaseous exchange with the atmosphere. The solutions are mainly over-saturated with respect to calcite, and over-saturation is all the more pronounced where the CO_2 pressure is small (S_{calcite} maximum ≈ 0.5). This process has been described by Al-Droubi (1976), Dosso (1980), and Gac (1980), and some authors attribute it to the presence of calcites of varying solubility as a result of more or less perfect crystallization. Valles (1987) attributed it to release of CO_2 without any precipitation of calcite, the rate of release being greater than that of the precipitation of large, well crystallized crystals of calcite. This discrepancy between release and precipitation rates is traditionally noted in both subterranean (e.g. Lastenet, 1994) and surface rivers (e.g. Ribolzi *et al.*, 1996), where agitation of the water encourages loss of CO_2 . It is probable that both phenomena occur with the water beneath the plateau. The rapid groundwater dynamics

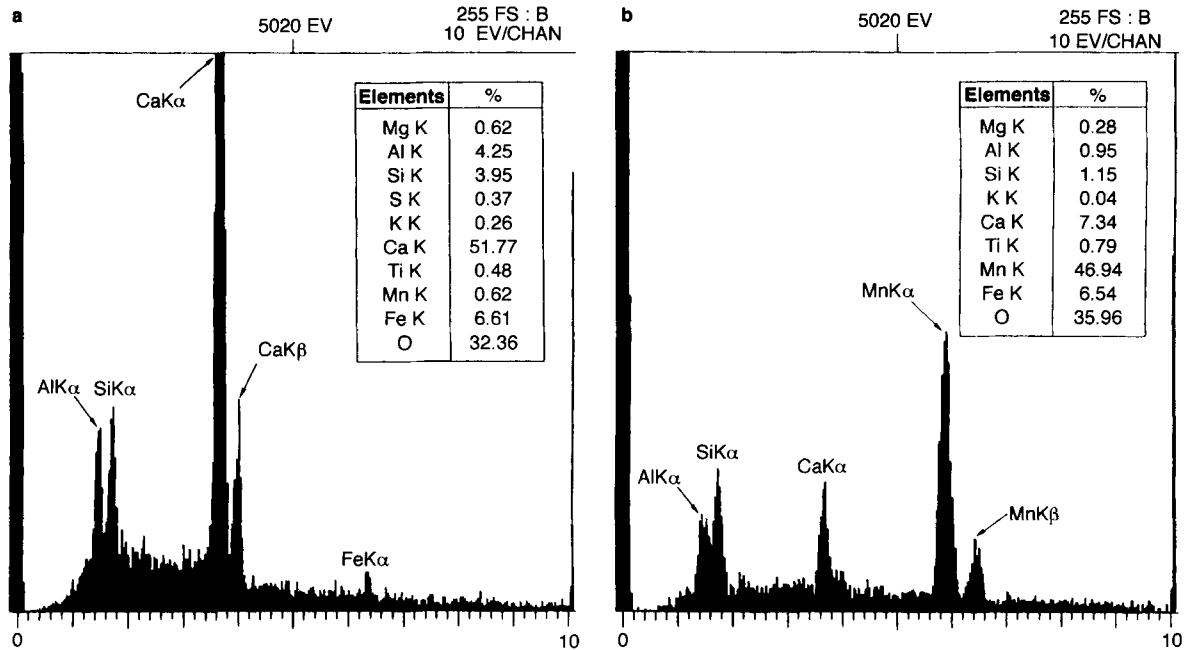


Fig. 4 Chemical composition of morphological features deduced from the electron microprobe analysis: (a) small crystals of calcite (P1, depth 120 cm), (b) black nodules of manganese (P2, depth 120 cm).

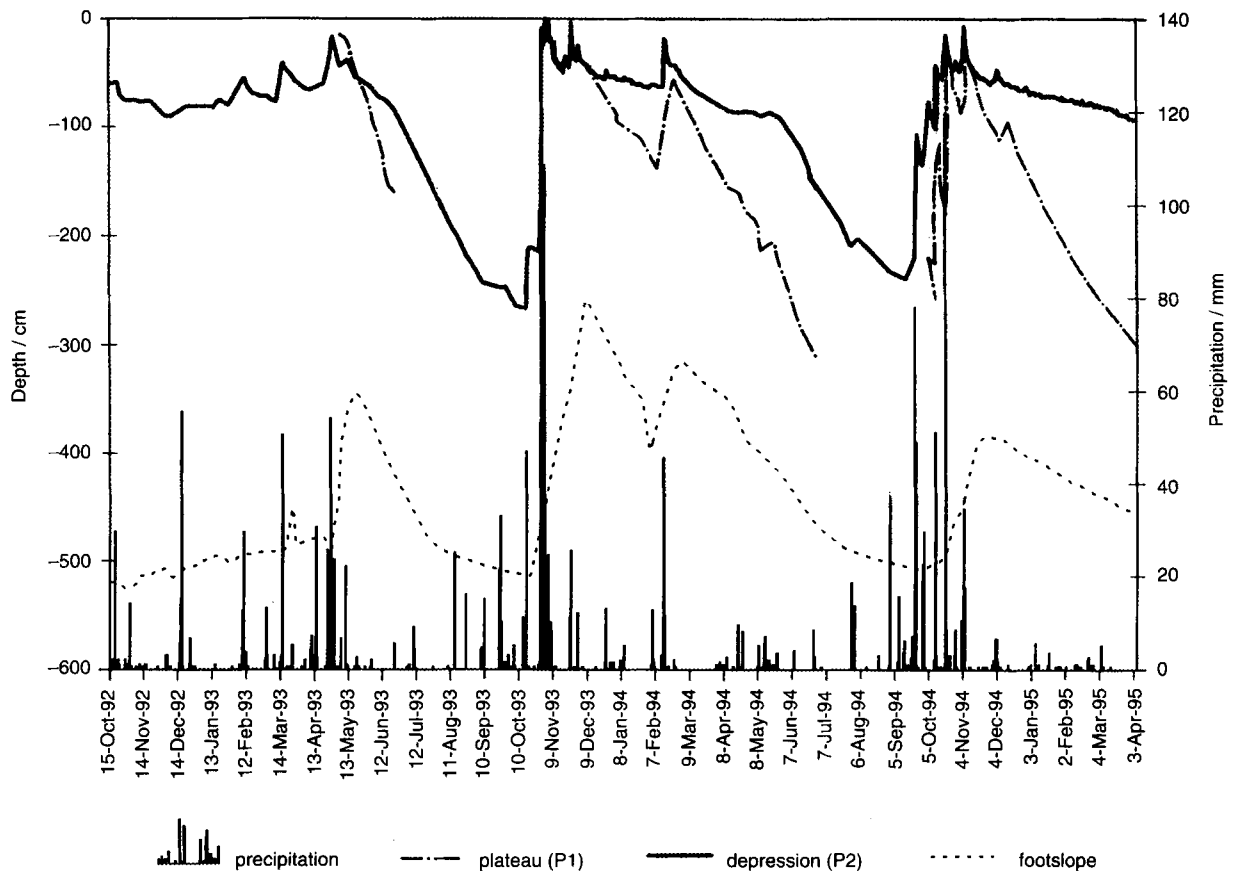


Fig. 5 Precipitation and groundwater fluctuations at the three sites studied.

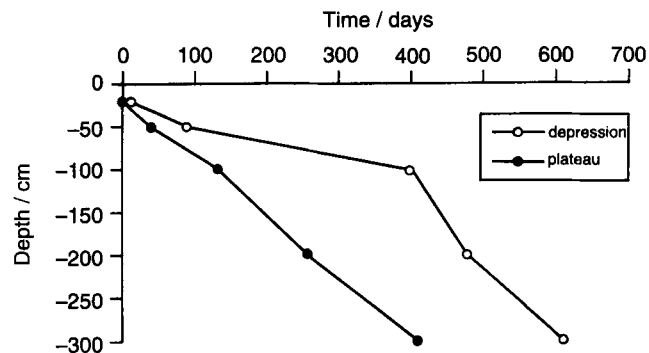


Fig. 6 Variation in groundwater persistence in relation to soil depth between 1 August 1993 and 5 April 1995.

encourage release of CO_2 , whilst extraction of water by plants not only lowers the water table but also dries the pore space and leads to a progressive concentration of the soil solution. This causes rapid over-saturation in respect of calcite, favouring nucleation and the formation of small crystals according to Equations (3) and (4) (Ostwald–Freundlich's law). For observed S_{calcite} values of 0.5 and an interfacial energy of 0.2 J m^{-2} , a radius of $0.01 \mu\text{m}$ is obtained, which indicates that the solutions are in equilibrium with crystals smaller than $1 \mu\text{m}$. In these conditions crystals of several

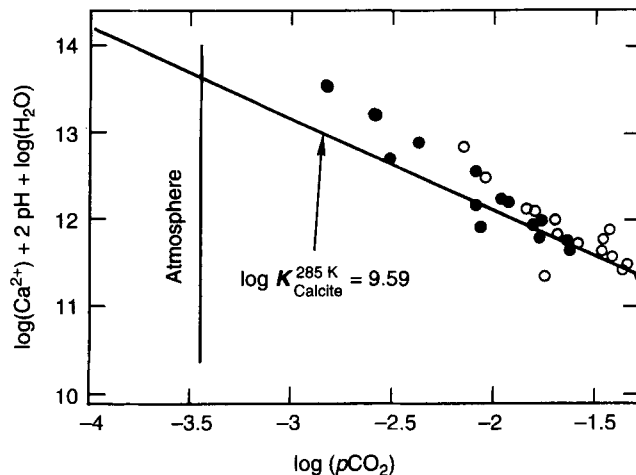


Fig. 7 Saturation diagram with respect to calcite (Ribolzi *et al.*, 1993) according to Equation (2). Groundwater solutions of the depression (○) and of the plateau with its border (●).

micrometres in size are stable. These observations explain the abundance of poorly crystallized micrites in the plateau soils, where the coarse pore space dries rapidly.

As the groundwater of the plateau provides only a slight reducing environment, only manganese can be mobilized. This result agrees with the presence at 50 cm depth or below

Table 1 Some physical (a) and chemical (b) properties of two profiles

(a) *P	Depth /cm	Clay	Sif	Sic	Saf	Sac	Om	N	pH in H ₂ O
		Particle size distribution /g kg ⁻¹					/g kg ⁻¹		
P1	0–50	332	152	51	256	209	10	7.0	8.1
	50–80	342	204	73	196	185	4	3.6	8.3
	80–120	353	180	82	227	158	2	2.8	8.2
	120–160	374	214	54	180	178			8.2
P2	0–50	270	259	181	218	72	11	8.9	8.2
	50–80	383	396	146	54	21	13	10.2	8.3
	80–100	255	196	181	310	58	6	4.7	8.3
	100–160	272	194	156	300	78	7	4.8	8.3
(b) *P	Depth /cm	CaCO ₃ /g kg ⁻¹	Ca ²⁺	Mg ²⁺	K ⁺	Na ⁺	CEC	Fe(d)	Fe(t)
			/mmol _c kg ⁻¹				/g kg ⁻¹		
P1	0–50	110	433	120	42	07	157	12.1	22.7
	50–80	293	458	102	30	12	181	11.5	22.6
	80–120	270	464	105	28	14	154	12.7	24.7
	120–160	284	479	103	34	33	171	13.7	26.3
P2	0–50	186	428	138	33	08	144	8.9	23.7
	50–80	192	483	292	30	25	184	12.9	32.2
	80–100	83	394	234	26	19	112	8.3	21.7
	100–160	54	405	318	30	21	136	7.0	22.2

(a) *P, profile studied; Clay, < 2 μm ; Sif, fine silt 2–20 μm ; Sic, coarse silt 20–50 μm ; Saf, fine sand 50–200 μm ; Sac, coarse sand 200–2000 μm ; Om, organic matter.

(b) *P, profile studied; CaCO₃, total CaCO₃; CEC, cation exchange capacity; Fe(d), free iron (Deb method); Fe(t), total Fe (extracted by HF).

Table 2 Variations with the time of estimated partial pressures expressed as $\log(pO_2)$ and $\log(pCO_2)$ near sites P1 and P2

Date	Plateau (P1)		Depression (P2)	
	$\log(pO_2)$	$\log(pCO_2)$	$\log(pO_2)$	$\log(pCO_2)$
24 March 1992	-19.51	-1.67	-25.85	-1.45
22 April 1992	-21.86	-1.78	-28.24	-1.62
5 May 1992	-25.85	-1.86	-24.05	-1.53
15 June 1993	ND	ND	-28.92	-1.33
12 January 1993	-27.48	-1.96	-28.20	-1.45
27 January 1993	-25.96	-2.17	-34.86	-1.48
3 February 1993	-23.29	-1.99	-35.62	-1.46

ND, not determined.

of pellicular manganiferous deposits. These cover reddish aggregates, indicating that they could have been produced only after rubefaction (Bornand, 1987). As in acid environments, manganese is thus a reliable indicator of hydromorphic conditions (Gotoh & Patrick, 1972).

The soils of the depression

As on the plateau, the groundwater beneath the depression remains only temporarily above 50 cm. It stays longer between 50 and 100 cm, however, and is almost permanent below this. The groundwater's presence leads to more pronounced anoxia than on the plateau, the estimated pCO_2 being up to 100 times that of the atmosphere. At 160 cm and below the soil is saturated with water near the theoretical equilibrium with calcite ($S_{\text{calcite}} \approx 0$). These conditions explain the presence of large rhombohedral crystals that regularly develop as saturation approaches zero. They grow in the fine pore space of the deep horizons where temporal variations in the chemical composition of the soil solution are slight (Valles, 1987). The large stable rhomboids in the nodules of calcite are associated

with a few small soluble crystals that dissolve when the groundwater is recharging, feeding the large crystals and contributing to the latter's gradual development.

Distribution of the rhizomorphic cells of calcite is uneven and varies from one kind of soil to another. These cells are more abundant in the grey horizon in the depression between 80 and 160–180 cm. This type of calcite within cells is characteristic of weak gaseous exchanges, notably of CO_2 (Jaillard *et al.*, 1991), which diffuses slowly because of the presence of the groundwater. A few calcitized cells also occur in the footslope soils, but only in very compact layers.

As far as metallic elements are concerned, the redox potential of the groundwater favours the precipitation of noncrystallized manganiferous nodules, whilst the long duration of saturation explains the small chroma values (Evans & Franzmeier, 1988).

Conclusion

The forms of carbonate redistribution enable us to infer the water regimes in calcareous soils of Mediterranean environments differing greatly in terms of age and structural organization. The redistribution and forms for iron and manganese provide additional clues. Observations can be combined with geochemical analyses and piezometric measurements to confirm the propriety of the criteria used to characterize soil water regimes.

The size of calcite crystals and their degree of crystallinity indicate the behaviour of the water table and duration of saturation. Rapid lowering leads to the formation of small, poorly crystallized crystals of calcite. Conversely, nearly permanent saturation is reflected in the development of nodules with large crystals of calcite. Rhizomorphic structures have no specific role as indicators of water excess. The latter is indicated much more by the abundance of these structures than

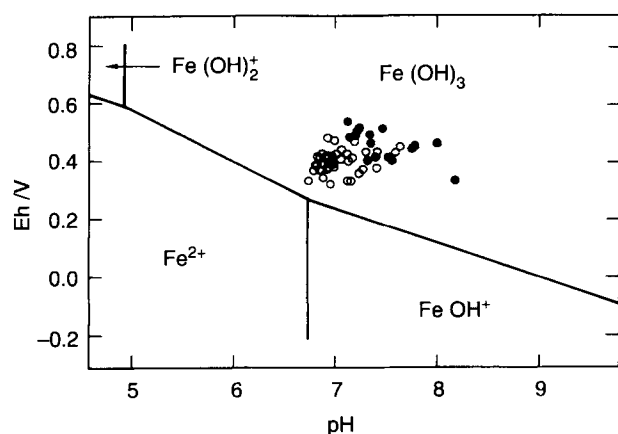


Fig. 8 Eh-pH diagram of dissolved iron species. Groundwater solutions of the depression (○) and of the plateau with its border (●).

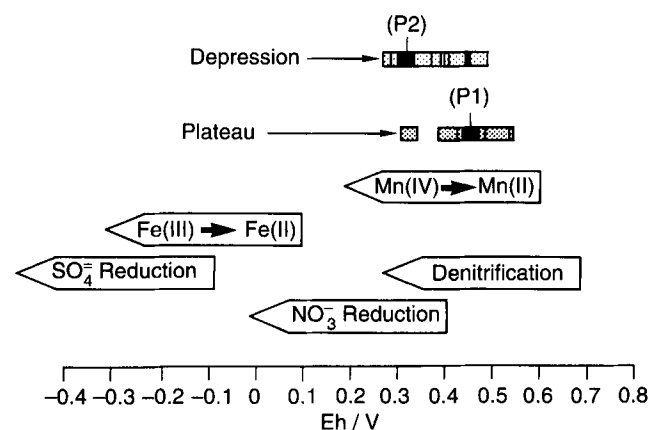


Fig. 9 Sequences of important redox processes at pH 7 in natural systems (modified from Stumm & Morgan, 1981), and redox potentials of groundwaters in the depression and of the plateau.

by their mere presence, which is also possible in nonwater-logged soils.

The features associated with iron and more particularly with manganese provide information only on the height of the water table.

Acknowledgements

We thank Patrick Andrieux and Marc Voltz, coordinators of the ALLEGRO-Roujan programme financed by INRA (AIP: 'Valorisation and protection de la ressource en eau'), and the Provence-Alpes-Côte d'Azur Region for its financial support. We also thank Garth Evans, who translated this article.

References

- Al-Droubi, A. 1976. *Géochimie des sels et des solutions concentrées par évaporation. Modèle thermodynamique de simulation Application aux sols salés du Tchad*. Thèse de doctorat Université Louis Pasteur, Strasbourg.
- Andrieux, P., Bouzigues, R., Joseph, C., Voltz, M., Lagacherie, P. & Bourlet, M. 1993. *Le bassin versant de Roujan. Caractéristiques générales du milieu*. INRA-UFR Science du Sol, Montpellier.
- Bornand, M. 1987. Transformation d'un cailloutis au cours du Quaternaire. *Genèse des paléosols associés (Vallée du Rhône)*. In: *Micromorphologie des Sols* (eds N. Fedoroff, L. M. Bresson & M. A. Courty), pp. 569–576. Association Française pour l'Etude du Sol, Plaisir.
- Bourrie, G. 1976. Relations entre le pH, l'alcalinité, le pouvoir tampon et les équilibres de CO₂ dans les eaux naturelles. *Science du Sol*, **14**, 141–159.
- Bouzigues, R., Favrot, J.C., Herrera, J. & Cid, G. 1992. Valeur diagnostique des caractères hydromorphes et halomorphes de vertisols de la vallée du Cauto à Cuba. Application à l'évaluation des besoins en drainage. *Cahiers de l'ORSTOM, Sene Pédologie*, **27**, 297–313.
- Crown, P. & Hoffman, D.W. 1970. Relationship between water table levels and type of mottles in four Ontario Gleysols. *Canadian Journal of Soil Science*, **50**, 453–457.
- Defay, R. & Prigogine, I. 1951. *Tension superficielle et adsorption*. Desoer, Liège.
- Delmas, A.B., Berrier, J. & Chamayou, H. 1987. Les figures de corrosion de la calcite: Typologie et séquence évolutives. In: *Micromorphologie des Sols* (eds N. Fedoroff, L. M. Bresson & M. A. Courty), pp. 303–308. Association Française pour l'Etude du Sol, Plaisir.
- Dosso, M. 1980. *Géochimie des sols salés et des eaux d'irrigation—Aménagement de la basse vallée de L'Euphrate en Syrie*. Thèse de doctorat, Institut National Polytechnique, Toulouse.
- Evans, C.V. & Franzmeier, D.P. 1988. Color index values to represent wetness and aeration in some Indiana soils. *Geoderma*, **41**, 353–368.
- Fanning, D.S., Hall, R.L. & Foss, J.E. 1973. Soil morphology, water table and iron relationships in soil of the Sassafras drainage catena in Maryland. In: *Pseudogley and Gley* (eds E. Schlichting & U. Schwertmann), pp. 71–79. Verlag Chemie GmbH, Weinheim.
- FAO, 1988. *Soil Map of the World, Revised Legend*. World Resources Report No 60. FAO, Rome.
- Faulkner, S.P. & Patrick, W.H. 1992. Redox processes and diagnostic wetland soil indicators in bottomland hardwood forests. *Soil Science Society of America Journal*, **56**, 856–865.
- Fritz, B. 1981. Etude thermodynamique et modélisation des réactions hydrothermales et diagénétiques. *Mémoire des Science Géologiques*, **65**, 1–197.
- Gac, J.Y. 1980. *Géochimie du bassin du lac Tchad*. ORSTOM, Paris.
- Garcia, B. 1996. *Etude des mécanismes de distribution spatiale des formes minérales de l'azote dans un aquifère. Application à la plaine alluviale méditerranéenne de la Vistrenque (Gard—France)*. Thèse de doctorat, Ecole Nationale du Génie Rural des Eaux et des Forêts, Montpellier.
- Gotoh, S. & Patrick, W.H. 1972. Transformation of manganese in a waterlogged soil as affected by redox potential and pH. *Soil Science Society of America Proceedings*, **36**, 738–742.
- Gran, G. 1952. Determination of the equivalence point in potentiometric titrations, Part II. *The Analyst*, **77**, 661–671.
- Hardan, A. & Abbas, A.K. 1973. Mechanisms of accumulation and distribution of calcium carbonate in marsh soils of the lower Mesopotamian Plain. In: *Pseudogley and Gley* (eds E. Schlichting & U. Schwertmann), pp. 123–130. Verlag Chemie GmbH, Weinheim.
- Helgeson, H.C. 1996. Thermodynamic of hydrothermal systems elevated temperatures and pressures. *American Journal of Science*, **267**, 724–804.
- Helgeson, H.C., Jones, J.A., Mundt, T., Brown, T., Nigrini, H.A., Leeper, R.H. & Kirkham, D.H. 1971. Path 1 and data bank PATDAT. *Computer Library Program No 1000*. University of California, Berkeley.
- Jaillard, B., Guyon, A. & Maurin, A.F. 1991. Structure and composition of calcified roots, and their identification in calcareous soils. *Geoderma*, **50**, 197–210.
- Kaemmerer, M., Revel, J.-C. & Barlier, J.-F. 1991. Formation des amas friables et des nodules calcaires dans des sols argileux en régions tempérée et semi-aride. *Science du Sol*, **29**, 1–12.
- Kaemmerer, M. & Revel, J.-C. 1996. New data on the laminar horizon genesis of calcretes developed on Morocco coarse Quaternary alluvium: Consequences on the desertification process. *Arid Soil Research and Rehabilitation*, **10**, 107–123.
- Keller, C., Bourrié, G. & Védry, J.-C. 1987. Formes de l'alcalinité dans les eaux gravitaires. Influence des métaux lourds contenus dans des composts. *Science du Sol*, **25**, 17–29.
- Lastenet, R. 1994. *Rôle de la zone non saturée dans le fonctionnement des aquifères karstiques, Approche par l'étude physico-chimique et isotopique du signal d'entrée et des exutoires du Massif Ventoux (Vaucluse)*. Thèse de doctorat, Université des Sciences, Avignon.
- Marlet, S. 1996. *Alcalinisation des Sols dans la Vallée du Fleuve Niger (Niger)*. Thèse de doctorat, Ecole Nationale Supérieure Agronomique, Montpellier.
- Mokma, D.L. & Sprecher, S.W. 1994a. Water table depths and color patterns in Spodosols of two hydrosequences in northern Michigan, USA. *Catena*, **22**, 275–286.
- Mokma, D.L. & Sprecher, S.W. 1994b. Water table depths and color patterns in soils developed from red parent materials in Michigan, USA. *Catena*, **22**, 287–298.
- Patrick, W.H. & Jugsujinda, A. 1992. Sequential reduction and oxidation of inorganic nitrogen, manganese, and iron in flooded soil. *Soil Science Society of America Journal*, **56**, 1071–1073.

- Ribolzi, O., Valles, V. & Barbiéro, L. 1993. Contrôle géochimique des eaux par la formation de calcite en milieu méditerranéen et en milieu tropical. Arguments d'équilibre et arguments de bilan. *Science du Sol*, **31**, 77–95.
- Ribolzi, O., Valles, V. & Bariac, T. 1996. Comparison of hydrograph deconvolutions using residual alkalinity, chloride and oxygen 18 as hydrochemical tracers. *Water Resources Research*, **32**, 1051–1059.
- Rieux, M. 1978. *Éléments d'un modèle mathématique de prédiction de la salure dans les sols irrigués. Application aux polders du Tchad*. Thèse de doctorat, Université Paul Sabatier, Toulouse.
- Sierra, J., Renault, P. & Valles, V. 1995. Anaerobiosis in saturated soil aggregates: modelling and experiment. *European Journal of Soil Science*, **46**, 519–531.
- Soulier, A. 1995. *Les formes solides du fer dans les sols hydromorphes. Approche géochimique, micromorphologique et minéralogique*. Thèse de doctorat, Ecole Nationale Supérieure Agronomique, Rennes.
- Stumm, W. & Morgan, J.J. 1981. *Aquatic Chemistry*. Wiley-Interscience, New York.
- Trambouze, W. 1996. *Caractérisation et éléments de modélisation de l'évapotranspiration réelle de la vigne à l'échelle de la parcelle*. Thèse de doctorat, Ecole Nationale Supérieure Agronomique, Montpellier.
- Valles, V. 1987. Modélisation des transferts d'eau et de sels dans un sol argileux—Application au calcul des doses d'irrigation. *Mémoire des Sciences Géologiques*, **79**, 1–148.
- Valles, V. & Bourgeat, F. 1988. Geochemical determination of gypsum requirement of cultivated sodic soils. I. Development of the thermodynamic model GYPSOL simulating the irrigation water–soil chemical interactions. *Arid Soil Research and Rehabilitation*, **2**, 165–177.
- Valles, V. & De Cockborne, A. F. 1992. Elaboration d'un logiciel de géochimie appliqué à l'étude de la qualité des eaux. In: *Colloque Altération et Restauration de la Qualité des Eaux Continentales* (ed. P. Legrand), pp. 27–30. INRA, dossiers de la cellule Environnement, Port-Leucate.
- Van Vallemburg, C. 1973. Hydromorphic soil characteristics in connection with soil drainage. In: *Pseudogley and Gley* (eds E. Schlichting & U. Schwertmann), pp. 393–403. Verlag Chemie GmbH, Weinheim.
- Vizier, J.-F. 1974. Contribution à l'étude de phénomènes d'hydromorphie. Recherche de relations morphogénétiques existant dans un type de séquence de sols hydromorphes peu humifères au Tchad. *Cahiers de l'ORSTOM, Série Pédologie*, **12**, 171–206.
- Vizier, J.-F. 1989. Étude du fonctionnement des milieux saturés d'eau. Une démarche physico-chimique. *Cahiers de l'ORSTOM, Série Pédologie*, **25**, 431–442.
- Vorob'yeva, A. & Zamana, S. P. 1984. The nature of soil alkalinity and methods of determining it. *Pochvovedeniye*, 1984(3), 134–139.